Supplementary figure 1. iPSC characterisation of pluripotency.

(A) Immunofluorescence staining at Day 16 of the Spontaneous in vitro differentiation protocol. SOX17 (SRY-BOX 17; endoderm-related), TUJ1 (Neuronal Class III β-Tubulin; ectoderm-related), and SMA (Alpha Smooth Muscle Actin; mesoderm-related) markers are shown. Nuclei were counterstained with DAPI. Scale bar, 500 µm. n=1 biological replicate per line.

(B) Immunofluorescence for pluripotency markers NANOG, OCT4, TRA-1-60, TRA-1-81 in iPSC lines. Nuclei were counterstained with DAPI. Scale bar, 200 µm. n=1 biological replicate per line.

(C) Epi-Pluri-Score testing for iPSC lines. DNA methylation profiles (β-values) in genes ANKRD46, C14orf115, and POU5F1 for all iPSC lines match profiles of pluripotent samples (red cloud). n=1 biological replicate per line.

(D) RT PCR in iPSC lines for expression of pluripotency markers SOX2, KLF4, NANOG, OCT4. H9 human embryonic stem cell (H9 hESC) line and human dermal fibroblasts were used as positive and negative controls, respectively. GAPDH was used as a housekeeping gene. n=1 biological replicate per line.

(E) RT PCR in iPSC lines for detection of Sendai virus genome and pluripotency transgenes. A positive (+ve) control (SeV DNA) and a negative control (cDNA from the H9 human embryonic stem cell line, H9 hESC) were also analysed. GAPDH was used as a housekeeping gene. n=1 biological replicate per line.

(F) Chromatograms from genomic DNA sequencing in BPAN iPSC lines. iPSC lines maintain disease-causing mutations. WDR45 disease-causing mutations are highlighted in the red rectangles. n=1 biological replicate per line.

(G) SNP array analysis of all iPSC lines used for downstream experiments, including the two isogenic controls. Representative images. All deletions/ gains in iPSCs used

for downstream experiments were small (<5Mb) and deemed as non-pathogenic by BlueFuse Multi. n=1 biological replicate per line.

(H) Alignment of wild type, patient 02 (c.19C>T), patient 03 (c.700C>T) and CRISPR corrected WDR45 genomic DNA (above) and amino acid (below) sequences. Premature protein truncation results from both c.19C>T and c.700C>T mutations. For each CRISPR-corrected line, three nucleotide substitutions have occurred after HDR (red rectangles). For both corrections, the first two are silent/ synonymous changes and, overall, the sequence leads to translation of a full-length WDR45 protein.

Supplementary Figure 2. Generation and basic characterisation of mDA model.

(A) Protocol for A9-type mDA differentiation.

(B) Immunofluorescence for ventral midbrain progenitor-specific markers FOXA2 and LMX1A at Day 11 of mDA differentiation. Nuclei were counterstained with DAPI. Scale bar, 500 µm. n=3 biological replicates per line.

(C) Quantification of FOXA2 and LMX1A abundance in Day 11 progenitors. n=3 biological replicates for all lines, 3 individual images from random areas of a well for each biological replicate. Percentages were calculated after manual counting of cells on ImageJ/Fiji (approximately 500 nuclei counted per image, followed by counting of cells also staining positive for FOXA2 and/or LMX1A).

(D) qRT-PCR at d11 for pluripotency markers OCT4 and NANOG, and midbrain related markers FOXA2, LMX1A, LMX1B, EN1, EN2, relative to housekeeping gene (GAPDH) and normalised to their respective iPSCs (n = 1 for each line, 3 technical replicates). Error bars indicate the Standard Error of Mean.

(E) qRT-PCR for TH, SNCA, NURR1, DAPT and DAT at day 65. mRNA values are relative to the housekeeping gene and normalised to the corresponding iPSCs (n = 3-5 per line).

(F) Cropped immunoblot of total WDR45 and beta actin protein expression at Day 11, and relevant quantification. n=3-4 biological replicates for each line.

Error bars represent the Standard Error of Mean. Statistics were calculated using ANOVA. Abbreviations: EBs= embryoid bodies. FC= fold change

Supplementary Figure 3. RNASeq at Day 65 of differentiation

(A) List of differentially expressed genes when comparing Patient 01, Patient 02, Patient 03 versus Control 01, Control 02, CRISPR 01 and CRISPR 02 mDA neurons.

(B) ClueGO analysis of GO terms enrichment of differentially expressed genes, showing pie charts for cellular component (CC), and molecular function (MF).

(C) Volcano plots of differentially expressed genes when comparing Patient 02 and corresponding CRISPR line (CRISPR 01), as well as Patient 03 versus corresponding CRISPR line (CRISPR 02). The top 40 genes (as per lowest p-values) are labelled. Right: GO Term and KEGG pathway enrichment analysis depicting intracellular pathways jointly corrected in both Patients 02 and 03, when compared to CRISPR 01 and 02.

(D) List of intracellular pathways and genes corrected in both Patients 02 and 03, when compared to CRISPR 01 and 02.

(E) List of differentially expressed genes and involved pathways when comparing Patient 02, versus CRISPR 01 (Patient 02 Corrected) and Patient 02 Torin 1- and Digoxin-treated mDA neurons.

(F) ClueGO analysis of GO terms enrichment of differentially expressed genes, showing pie charts for cellular component (CC), and molecular function (MF).

n=3 for all lines, median TPM values analysed. Network graph nodes represent GO terms (the most significant are named) and edges indicate shared genes between GO terms. Functional groups of GO terms are indicated by the same colour. Pie charts show the percentages of each functional group representation. GO functional groups exhibiting statistically significant differences ($p < 0.05$) are shown.

Supplementary Figure 4. Defective autophagy flux in BPAN cells.

(A) Patient and control fibroblasts imaged after 3-hour treatments with DMSO, autophagy flux inducers (Torin 1) and/ or inhibitors (Bafilomycin A1). Representative images. Cells were plated in 96-well plates at a density of 15,000 cells/well. n=5 biological replicates for each line. For each biological replicate, all lines were seeded on the same 96-well plate.

(B) Quantification of LC3 puncta/ nuclei in control and patient-derived fibroblasts. For statistical analysis, the Student's unpaired two tailed t-test was used. Error bars represent the Standard Error of Mean.

(C) Quantification of LC3 puncta/ nuclei in control and patient-derived neuronal progenitors, at basal (DMSO-treated) conditions. Experiment identical to the one depicted in Fig. 3A-B, but with more independent biological replicates (n=11). Additional replicates enhance the statistical significance of previous findings. For statistical analysis, the Student's unpaired two tailed t-test was used. Error bars represent the Standard Error of Mean.

(D) Day 11 ventral progenitors imaged after 3-hour autophagy flux induction or inhibition. Representative images. Cells were plated in 96-well plates at a density of 15,000 cells/well. n=7 independent differentiations/ biological replicates for each line. For each biological replicate, all 5 lines had the same start date of differentiation and were seeded on the same 96-well plate.

(E) Quantification of LC3 puncta/ nuclei in control and patient-derived neurons. For statistical analysis, the Student's unpaired two tailed t-test was used. Error bars represent the Standard Error of Mean.

Supplementary Tables

Supplementary Table 1. Fibroblast and corresponding iPSC lines used.

Fibroblast Identifier	iPSC clone used after characterisation	WDR45 mutation	Protein Effect	Age at biopsy	Gender
HDF7301	HDF7301-05 (Control 01)	Healthy Control	-	13y	F
582-202	582-06 (Control 02)	Healthy Control	-	1y10mo	M
BUCL01	BPAN07 (Patient 01)	c.344+2T>A	p.(Ile116Argfs*3)	5y	F
587-201A	587-02 (Patient 02)	c.19C>T	p.Arg7*	19y8mo	M
535-201	535-02 (Patient 03)	c.700C>T	p.Arg234*	6y4mo	F
	R7-72 (CRISPR 01, Patient 02 Corrected)	Substitution of c.19C>T with 'wild-type' sequence	Normal length	19y8mo	M
	R234-68 (CRISPR 02, Patient 03 Corrected)	Substitution of c.19C>T with 'wild-type' sequence	Normal length	6y4mo	F

After characterisation of pluripotency, one iPSC clone from each line was used for downstream differentiations. The first patient line (Patient 01, BPAN07) carries a splice site mutation that leads to aberrant splicing and an early stop codon. Alignment of wild type & WDR45 c.344+2T>A amino acid sequences shows premature truncation of the protein by 246 amino acids with the inclusion of 2 aberrant residues (arginine and Alanine); p.(Ile116Argfs*3) (data not shown). The other two patient lines (587-02 and 535-02) harbour nonsense pathogenic mutations leading to an early stop codon. In the isogenic controls R7-72 and R234-68, disease-causing mutations (in Patients 02 and 03, respectively) were corrected using CRISPR/Cas9-mediated genome editing (Supplementary Figure 1). Age- matched healthy control fibroblasts HDF-7301 were collected from the MRC Centre for Neuromuscular Disorders Biobank. Patient fibroblast line BUCL01 was ascertained from the University College London (UCL) Great Ormond Street Institute of Child Health (UCL GOS ICH), London, UK. Control fibroblast line 582-202 and patient lines 587-201A and 535-201 were obtained from Oregon Health and Science University (OHSU), Portland, Oregon, USA. Patient BUCL01 and control HDF-7301 fibroblasts were reprogrammed into iPSC at

UCL GOS ICH, while control 582-202 and patients 587-201A and 535-201 fibroblasts at the Wellcome Trust-Medical Research Council Cambridge Stem Cell Institute (Anne McLaren Laboratory for Regenerative Medicine, Cambridge, UK). Lines 587-02 and 535-02 (as well as the isogenic controls R7-72 and R234-68) were initially plated on Vitronectin XF (Stemcell Technologies)-coated plates and cultured in TeSR-E8 (StemCell Technologies). These lines were subsequently transferred to Matrigel/ mTeSR1 culture conditions.

Supplementary Table 2. sgRNA and HDR donor templates used for CRISPR/Cas9 genome editing in patient lines.

Patient 02 (iPSC clone 587-02); c.19C>T	
sgRNA 1	ATGACTCAACAGCCACTTTG AGG (reverse strand)
sgRNA2	AGGCTGGTCACTCCTCAAAG TGG (forward strand)
HDR donor template	C*T*C*TCTCACTTTGGTCTTGGTTGAAACGCAGGC TGGTCACTCCTCGTAATGGCTGTTGAGTCATGGTG CAGGATTGTTCCTCTGCAT*A*C*A
Patient 03 (iPSC clone 535-02); c.700C>T	
sgRNA 1	AAACTGGTGGAGCTGCGCTG AGG (reverse strand)
HDR donor template	C*A*T*ACCCTGTGCTCACCAGTAGAGGGTGGCAG GGTCAGTGCCTCGTCTCAGCTCCACCAGTTTCTCC TTGGATTGTGTGTCAAAGAG*G*C*G

CRISPR/Cas9-mediated mutation correction in Patient 02 (clone 587-02) and Patient 03 (clone 535-02) iPSC lines was performed at the Wellcome Trust-Medical Research Council Cambridge Stem Cell Institute. sgRNA= single guide RNA, HDR= Homology-Directed Repair

Supplementary Table 3. PCR primers for WDR45 gene sequencing.

Exon	Size (bp)	Annealing Temp	Primer Sequence	
3 (Coding Exon 1)	261	55°C	3F	TCCCAAAGTGCTGGATTAC
			3R	TTCCTCCCACAAGGGTACAG
4-5 (Coding Exons 2-3)	429	60°C	4-5F	CTGTACCCTTGTGGGAGGAA
			4-5R	CCAGGAATCCGAGAAATCTG
6-7 (Coding Exons 4-5)	505	60°C	6-7F	GCCCCTTACCCTAAACCTTG
			6-7R	TGAGTGTGAGCATCTCCCTG
8-9 (Coding Exons 6-7)	596	60°C	8-9F	TCTGGTCCTCATCCAGCTCT
			8-9R	CAGAGGAAGGAGGAGTCGTG
10-11 (Coding Exons 8-9)	707	60°C	10-11F	GTCTGCTCCATTCACGATCA
			10-11R	GCTGTCCCCCTTACTGATGA
12 (Coding Exon 10)	634	60°C	12F	AGATGCCTGAGAGGACTGGA
			12R	AATCCCCAGGTTGGATTAGG

Tm= annealing temperature. F= forward, R= reverse

Supplementary Table 4. Primers used for WDR45 cDNA sequencing.

Exons	Expected size	Primers used		Coverage
1-4	391bp	F	GACTCAACAGCCACTTCGAGGA	Beginning of Exon 3 to mid-Exon 7
		R	GTCGGGGAAGGAGTACACAT	
5-7	465bp	F	AGCTAAGCGCGAGAAGGCGTTCACCTTCACCAAGCCAG	Late Exon 6 to Exon 10
		R	GCTTTACCGCTCAACCGTTCAGAGGAAGGAGGAGTCGTG	
8-10	675bp	F	GTGTACTCCTTCCCCGACAA	Mid-exon 7 to mid-exon 12
		R	CGTCGAAAGCCTCTCTGTTG	

F= forward, R= reverse

Supplementary Table 5. Primer pairs for detection of pluripotency marker expression via RT PCR.

Primer name	Sequence (5'-3')	PCR product size (bp)
GAPDH F	ATCCCATCACCATCTTCCAG	382
GAPDH R	CCATCACGCCACAGTTTCC	
OCT4 F	CGAAACCCACACTGCAGCAG	402
OCT4 R	CCTGGCACAAACTCCAGGTTT	
SOX2 F	GGGAAATGGGAGGGGTGCAAAAGAGG	151
SOX2 R	TTGCGTGAGTGTGGATGGGATTGGTG	
NANOG F	CAGCCCCGATTCTTCCAGTCCC	343
NANOG R	CGGAAGATTCCCAGTCGGGTTCACC	
c-MYC F	GCGTCCTGGGAAGGGAGATCCGGAGC	328
c-MYC R	TTGAGGGGCATCGTCGCGGGAGGCTG	
KLF4 F	ATATCCCGCCGTGGGTGAAAGTTC	243
KLF4 R	ACTCAGCCATGGACTGGAGCATCC	

F= forward, R= reverse

Supplementary Table 6. Primers used for Sendai Virus Clearance-related RT PCR experiments.

Primer name	Sequence (5'-3')	PCR product size (bp)
SeV F	GGATCACTAGGTGATATCGAGC	181
SeV R	ACCAGACAAGAGTTTAAGAGATATGTATC	
SeV SOX2 F	ATGCACCGCTACGACGTGAGCGC	451
SeV SOX2 R	AATGTATCGAAGGTGCTCAA	
SeV KLF4 F	TTCCTGCATGCCAGAGGAGCCC	410
SeV KLF4 R	AATGTATCGAAGGTGCTCAA	
SeV c-MYC F	TAACTGACTAGCAGGCTTGTCG	532
SeV c-MYC R	TCCACATACAGTCCTGGATGATGATG	
SeV OCT4 F	CCCGAAAGAGAAAGCGAACCAG	483
SeV OCT4 R	AATGTATCGAAGGTGCTCAA	
GAPDH F	ATCCCATCACCATCTTCCAG	382
GAPDH R	CCATCACGCCACAGTTTCC	

F= forward, R= reverse, SeV= Sendai Virus

Supplementary Table 7. qRT PCR primers used for Day 11 and Day 65 characterisation.

qRT PCR primers	
Primer name	**Sequence (5'-3')**
GAPDH F	TTGAGGTCAATGAAGGGGTC
GAPDH R	GAAGGTGAAGGTCGGAGTCA
FOXA2 F	CCGTTCTCCATCAACAACCT
FOXA2 R	GGGGTAGTGCATCACCTGTT
EN1 F	CGTGGCTTACTCCCCATTTA
EN1 R	TCTCGCTGTCTCTCCCTCTC
EN2 F	CCTCCTGCTCCTCCTTTCTT
EN2 R	GACGCAGACGATGTATGCAC
LMX1A F	CGCATCGTTTCTTCTCCTCT
LMX1A R	CAGACAGACTTGGGGCTCAC
LMX1B F	CTTAACCAGCCTCAGCGACT
LMX1B R	TCAGGAGGCGAAGTAGGAAC
OCT4 F	TCTCCAGGTTGCCTCTCACT
OCT4 R	GTGGAGGAAGCTGACAACAA
NANOG F	TTGGGACTGGTGGAAGAATC
NANOG R	GATTTGTGGGCCTGAAGAAA
TH F	CGGGCTTCTCGGACCAGGTGTA
TH R	CTCCTCGGCGGTGTACTCCACA
DAT F	TCACCAACGGTGGCATCTAC
DAT R	CACTCCGATGGCTTCGATGA
NURR1 F	TGCGAGCAGAGAGGGAGTAG
NURR1 R	TCGACATTTCTGCCTTCTCCTG
SNCA F	GGAGTGGCCATTCGACGAC
SNCA R	CCTGCTGCTTCTGCCACAC
MAPT F	CTCGCATGGTCAGTAAAAGCAA
MAPT R	GGGTTTTTGCTGGAATCCTGGT
WDR45 F	TGCGCCATGACAAGATCGT
WDR45 R	ACTCAAACAGCTTTCGGGGAT

The following protocol was used on the StepOnePlus Real-Time PCR System: 1 cycle of 5 min (initial denaturation step) followed by 40 cycles at 95°C for 15 sec (denaturation) and at 60°C for 60 sec (annealing, extension). Abbreviations: F= forward; R= reverse

Supplementary Table 8. Primary and corresponding secondary antibodies used for immunofluorescence and western blotting experiments.

Western Blot Antibodies		
Primary Antibody	**Company/ Catalogue Number**	**Dilution**
Beta Actin mouse monoclonal antibody (clone AC-15)	Sigma (A1978)	1:4,000
LC3B rabbit polyclonal antibody	Sigma (L7543)	1:1,000
WDR45 rabbit monoclonal antibody	Gift from Professor Sharon Tooze's laboratory, Francis Crick Institute, London, UK	1:250
WDR45 rabbit polyclonal antibody	Proteintech (19194-1-AP)	1:2,000
Secondary Antibody	**Company/ Catalogue Number**	**Dilution**
Anti-mouse IgG, HRP-linked Antibody	Cell signalling technology (7076)	1:5,000
Anti-rabbit IgG, HRP-linked Antibody	Cell signalling technology (7074)	1:5,000
Immunofluorescence Antibodies		
Primary Antibody	**Company/ Catalogue Number**	**Dilution**
FOXA2 mouse monoclonal antibody	BD Pharmigen (561580)	1:500
LMX1A rabbit polyclonal antibody	Millipore (AB10533)	1:2,000
MAP2 Mouse monoclonal antibody	Sigma	1:400
NANOG Mouse monoclonal antibody	Millipore	1:500
OCT4 Mouse monoclonal antibody	Santa Cruz	1:50
SMA Rabbit monoclonal antibody	Abcam	1:100
SOX17 Goat polyclonal antibody	R&D Systems	1:200
TH Chicken polyclonal antibody	Aves	1:400
TRA-1-60 Mouse monoclonal antibody	Santa Cruz	1:200
TRA-1-81 Mouse monoclonal antibody	Millipore	1:200
TUJ1 Mouse monoclonal antibody	BioLegend	1:400
Secondary Antibody	**Company/ Catalogue Number**	**Dilution**
Alexa Fluor 488 Donkey Anti-Goat IgG	ThermoFisher (A-11055)	1:400
Alexa Fluor 488 Goat Anti-Mouse IgG	ThermoFisher (A-11001)	1:400
Alexa Fluor 488 Goat Anti-Rabbit IgG	ThermoFisher (A-11008)	1:400
Alexa Fluor 594 Goat Anti-Chicken IgG	ThermoFisher (A-11042)	1:400
Alexa Fluor 594 Goat Anti-Mouse IgM	Thermofisher (A-21044)	1:400
Alexa Fluor 594 Goat Anti-Rabbit IgG	ThermoFisher (A-11012)	1:400
High Content Immunofluorescence Antibodies		
Primary Antibody	**Company/ Catalogue Number**	**Dilution**
LC3B rabbit monoclonal antibody (clone D11)	Cell Signalling Technology (3868S)	1:200
P62/SQSTM1 rabbit polyclonal antibody	Sigma (P0067)	1:1,000
Secondary Antibody	**Company/ Catalogue Number**	**Dilution**
Alexa Fluor 488 Goat Anti-Mouse IgG	ThermoFisher (A-11001)	1:400
Alexa Fluor 488 Goat Anti-Rabbit IgG	ThermoFisher (A-11008)	1:400

Supplementary Table 9. Hits from Prestwick screen with the 200 highest z-scores.

1. Meyer E, Kurian MA, Hayflick SJ. Neurodegeneration with Brain Iron Accumulation: Genetic Diversity and Pathophysiological Mechanisms. *Annu Rev Genomics Hum Genet* **16**, 257-279 (2015).

2. Hayflick SJ, Kurian MA, Hogarth P. Neurodegeneration with brain iron accumulation. *Handbook of clinical neurology* **147**, 293-305 (2018).

3. Hayflick SJ*, et al.* beta-Propeller protein-associated neurodegeneration: a new X-linked dominant disorder with brain iron accumulation. *Brain* **136**, 1708-1717 (2013).

4. Haack TB*, et al.* Exome sequencing reveals de novo WDR45 mutations causing a phenotypically distinct, X-linked dominant form of NBIA. *American journal of human genetics* **91**, 1144-1149 (2012).

5. Saitsu H*, et al.* De novo mutations in the autophagy gene WDR45 cause static encephalopathy of childhood with neurodegeneration in adulthood. *Nature genetics* **45**, 445-449, 449e441 (2013).

6. Zhao YG*, et al.* The autophagy gene Wdr45/Wipi4 regulates learning and memory function and axonal homeostasis. *Autophagy* **11**, 881-890 (2015).

7. Bakula D*, et al.* WIPI3 and WIPI4 beta-propellers are scaffolds for LKB1-AMPK-TSC signalling circuits in the control of autophagy. **8**, 15637 (2017).

8. Proikas-Cezanne T, Takacs Z, Donnes P, Kohlbacher O. WIPI proteins: essential PtdIns3P effectors at the nascent autophagosome. *Journal of cell science* **128**, 207-217 (2015).

9. Paudel R*, et al.* Neuropathology of Beta-propeller protein associated neurodegeneration (BPAN): a new tauopathy. *Acta neuropathologica communications* **3**, 39 (2015).

10. Teinert J, Behne R, Wimmer M, Ebrahimi-Fakhari D. Novel insights into the clinical and molecular spectrum of congenital disorders of autophagy. *Journal of inherited metabolic disease*, (2019).

11. Choi AM, Ryter SW, Levine B. Autophagy in human health and disease. *The New England journal of medicine* **368**, 651-662 (2013).

12. Stead ER*, et al.* Agephagy - Adapting Autophagy for Health During Aging. *Frontiers in cell and developmental biology* **7**, 308 (2019).

13. Agrotis A, Ketteler R. On ATG4B as Drug Target for Treatment of Solid Tumours-The Knowns and the Unknowns. *Cells* **9**, (2019).

14. Agrotis A, von Chamier L, Oliver H, Kiso K, Singh T, Ketteler R. Human ATG4 autophagy proteases counteract attachment of ubiquitin-like LC3/GABARAP

proteins to other cellular proteins. *The Journal of biological chemistry* **294**, 12610-12621 (2019).

15. Baskaran S, Ragusa MJ, Boura E, Hurley JH. Two-site recognition of phosphatidylinositol 3-phosphate by PROPPINs in autophagy. *Molecular cell* **47**, 339-348 (2012).

16. Smith TF, Gaitatzes C, Saxena K, Neer EJ. The WD repeat: a common architecture for diverse functions. *Trends Biochem Sci* **24**, 181-185 (1999).

17. Li D, Roberts R. WD-repeat proteins: structure characteristics, biological function, and their involvement in human diseases. *Cell Mol Life Sci* **58**, 2085-2097 (2001).

18. Lu Q*, et al.* The WD40 repeat PtdIns(3)P-binding protein EPG-6 regulates progression of omegasomes to autophagosomes. *Dev Cell* **21**, 343-357 (2011).

19. Obara K, Sekito T, Niimi K, Ohsumi Y. The Atg18-Atg2 complex is recruited to autophagic membranes via phosphatidylinositol 3-phosphate and exerts an essential function. *The Journal of biological chemistry* **283**, 23972-23980 (2008).

20. Nakatogawa H, Suzuki K, Kamada Y, Ohsumi Y. Dynamics and diversity in autophagy mechanisms: lessons from yeast. *Nature reviews Molecular cell biology* **10**, 458-467 (2009).

21. Wan H*, et al.* WDR45 contributes to neurodegeneration through regulation of ER homeostasis and neuronal death. *Autophagy*, 1-17 (2019).

22. Seibler P*, et al.* Iron overload is accompanied by mitochondrial and lysosomal dysfunction in WDR45 mutant cells. *Brain*, (2018).

23. Fusaki N, Ban H, Nishiyama A, Saeki K, Hasegawa M. Efficient induction of transgene-free human pluripotent stem cells using a vector based on Sendai virus, an RNA virus that does not integrate into the host genome. *Proceedings of the Japan Academy Series B, Physical and biological sciences* **85**, 348-362 (2009).

24. Gasteiger E, Gattiker A, Hoogland C, Ivanyi I, Appel RD, Bairoch A. ExPASy: The proteomics server for in-depth protein knowledge and analysis. *Nucleic acids research* **31**, 3784-3788 (2003).

25. Lenz M*, et al.* Epigenetic biomarker to support classification into pluripotent and non-pluripotent cells. *Scientific reports* **5**, 8973 (2015).

26. Ng J*, et al.* Gene therapy restores dopamine transporter expression and ameliorates pathology in iPSC and mouse models of infantile parkinsonism. *Science translational medicine* **13**, (2021).

27. Kirkeby A*, et al.* Generation of regionally specified neural progenitors and functional neurons from human embryonic stem cells under defined conditions. *Cell reports* **1**, 703-714 (2012).

28. Tomoda K*, et al.* Derivation conditions impact X-inactivation status in female human induced pluripotent stem cells. *Cell Stem Cell* **11**, 91-99 (2012).

29. Tchieu J*, et al.* Female human iPSCs retain an inactive X chromosome. *Cell Stem Cell* **7**, 329-342 (2010).

30. Bar S, Seaton LR, Weissbein U, Eldar-Geva T, Benvenisty N. Global Characterization of X Chromosome Inactivation in Human Pluripotent Stem Cells. *Cell reports* **27**, 20-29.e23 (2019).

31. Mekhoubad S, Bock C, de Boer AS, Kiskinis E, Meissner A, Eggan K. Erosion of dosage compensation impacts human iPSC disease modeling. *Cell Stem Cell* **10**, 595-609 (2012).

32. Comertpay S*, et al.* Evaluation of clonal origin of malignant mesothelioma. *J Transl Med* **12**, 301 (2014).

33. Love MI, Huber W, Anders S. Moderated estimation of fold change and dispersion for RNA-seq data with DESeq2. *Genome biology* **15**, 550 (2014).

34. Mi H, Muruganujan A, Thomas PD. PANTHER in 2013: modeling the evolution of gene function, and other gene attributes, in the context of phylogenetic trees. *Nucleic acids research* **41**, D377-386 (2013).

35. The Gene Ontology resource: enriching a GOld mine. *Nucleic acids research* **49**, D325-d334 (2021).

36. Ashburner M*, et al.* Gene ontology: tool for the unification of biology. The Gene Ontology Consortium. *Nature genetics* **25**, 25-29 (2000).

37. Kanehisa M, Furumichi M, Tanabe M, Sato Y, Morishima K. KEGG: new perspectives on genomes, pathways, diseases and drugs. *Nucleic acids research* **45**, D353-d361 (2017).

38. Kanehisa M, Goto S, Furumichi M, Tanabe M, Hirakawa M. KEGG for representation and analysis of molecular networks involving diseases and drugs. *Nucleic acids research* **38**, D355-360 (2010).

39. Kanehisa M, Sato Y, Kawashima M, Furumichi M, Tanabe M. KEGG as a reference resource for gene and protein annotation. *Nucleic acids research* **44**, D457-462 (2016).

40. Jiao X*, et al.* DAVID-WS: a stateful web service to facilitate gene/protein list analysis. *Bioinformatics* **28**, 1805-1806 (2012).

41. Mitre M, Mariga A, Chao MV. Neurotrophin signalling: novel insights into mechanisms and pathophysiology. *Clin Sci (Lond)* **131**, 13-23 (2017).

42. Chen X, Yu C, Kang R, Tang D. Iron Metabolism in Ferroptosis. *Front Cell Dev Biol* **8**, 590226 (2020).

43. Wu Q, Maniatis T. A striking organization of a large family of human neural cadherin-like cell adhesion genes. *Cell* **97**, 779-790 (1999).

44. De Wolf V*, et al.* A complex Xp11.22 deletion in a patient with syndromic autism: exploration of FAM120C as a positional candidate gene for autism. *American journal of medical genetics Part A* **164a**, 3035-3041 (2014).

45. Nishimoto S, Kusakabe M, Nishida E. Requirement of the MEK5-ERK5 pathway for neural differentiation in Xenopus embryonic development. *EMBO Rep* **6**, 1064-1069 (2005).

46. Zou J*, et al.* Targeted deletion of ERK5 MAP kinase in the developing nervous system impairs development of GABAergic interneurons in the main olfactory bulb and behavioral discrimination between structurally similar odorants. *The Journal of neuroscience : the official journal of the Society for Neuroscience* **32**, 4118-4132 (2012).

47. Hetz C, Papa FR. The Unfolded Protein Response and Cell Fate Control. *Molecular cell* **69**, 169-181 (2018).

48. Brunetti-Pierri N, Scaglia F. GM1 gangliosidosis: review of clinical, molecular, and therapeutic aspects. *Molecular genetics and metabolism* **94**, 391-396 (2008).

49. Mohammad SS*, et al.* Magnetic resonance imaging pattern recognition in childhood bilateral basal ganglia disorders. *Brain Commun* **2**, fcaa178 (2020).

50. Regier DS*, et al.* MRI/MRS as a surrogate marker for clinical progression in GM1 gangliosidosis. *American journal of medical genetics Part A* **170**, 634-644 (2016).

51. Kukkonen JP. Orexin/Hypocretin Signaling. *Curr Top Behav Neurosci* **33**, 17-50 (2017).

52. Wilson JL*, et al.* Consensus clinical management guideline for beta-propeller protein-associated neurodegeneration. *Developmental medicine and child neurology*, (2021).

53. Lee JR. Protein tyrosine phosphatase PTPRT as a regulator of synaptic formation and neuronal development. *BMB Rep* **48**, 249-255 (2015).

54. Nam J, Mah W, Kim E. The SALM/Lrfn family of leucine-rich repeat-containing cell adhesion molecules. *Semin Cell Dev Biol* **22**, 492-498 (2011).

55. Pei YP*, et al.* ICAM5 as a Novel Target for Treating Cognitive Impairment in Fragile X Syndrome. *The Journal of neuroscience : the official journal of the Society for Neuroscience* **40**, 1355-1365 (2020).

56. Fernandez RF*, et al.* Acyl-CoA synthetase 6 enriches the neuroprotective omega-3 fatty acid DHA in the brain. *Proceedings of the National Academy of Sciences of the United States of America* **115**, 12525-12530 (2018).

57. Gottlieb RA, Andres AM, Sin J, Taylor DP. Untangling autophagy measurements: all fluxed up. *Circ Res* **116**, 504-514 (2015).

58. Yoshii SR, Mizushima N. Monitoring and Measuring Autophagy. *International journal of molecular sciences* **18**, (2017).

59. Mauthe M*, et al.* Chloroquine inhibits autophagic flux by decreasing autophagosome-lysosome fusion. *Autophagy* **14**, 1435-1455 (2018).

60. Pelz O, Gilsdorf M, Boutros M. web cellHTS2: a web-application for the analysis of high-throughput screening data. *BMC Bioinformatics* **11**, 185 (2010).

61. Waguri S, Komatsu M. Biochemical and morphological detection of inclusion bodies in autophagy-deficient mice. *Methods Enzymol* **453**, 181-196 (2009).

62. Kraja AT*, et al.* Associations of Mitochondrial and Nuclear Mitochondrial Variants and Genes with Seven Metabolic Traits. *American journal of human genetics* **104**, 112-138 (2019).

63. Liang C*, et al.* Autophagic and tumour suppressor activity of a novel Beclin1-binding protein UVRAG. *Nature cell biology* **8**, 688-699 (2006).

64. Agrotis A, Pengo N, Burden JJ, Ketteler R. Redundancy of human ATG4 protease isoforms in autophagy and LC3/GABARAP processing revealed in cells. *Autophagy* **15**, 976-997 (2019).

65. Barral S, Kurian MA. Utility of Induced Pluripotent Stem Cells for the Study and Treatment of Genetic Diseases: Focus on Childhood Neurological Disorders. *Frontiers in molecular neuroscience* **9**, 78 (2016).

66. Xiong Q*, et al.* WDR45 Mutation Impairs the Autophagic Degradation of Transferrin Receptor and Promotes Ferroptosis. *Front Mol Biosci* **8**, 645831 (2021).

67. Fu XH*, et al.* COL1A1 affects apoptosis by regulating oxidative stress and autophagy in bovine cumulus cells. *Theriogenology* **139**, 81-89 (2019).

68. Paiva I*, et al.* Alpha-synuclein deregulates the expression of COL4A2 and impairs ER-Golgi function. *Neurobiology of disease* **119**, 121-135 (2018).

69. Tang ME, *et al.* Matrix metalloproteinase-degraded type I collagen is associated with APOE/TOMM40 variants and preclinical dementia. *Neurology Genetics* **6**, e508 (2020).

70. Cescon M, Chen P, Castagnaro S, Gregorio I, Bonaldo P. Lack of collagen VI promotes neurodegeneration by impairing autophagy and inducing apoptosis during aging. *Aging (Albany NY)* **8**, 1083-1101 (2016).

71. Stanga D, Zhao Q, Milev MP, Saint-Dic D, Jimenez-Mallebrera C, Sacher M. TRAPPC11 functions in autophagy by recruiting ATG2B-WIPI4/WDR45 to preautophagosomal membranes. *Traffic (Copenhagen, Denmark)* **20**, 325-345 (2019).

72. Chang CY, *et al.* Induced Pluripotent Stem Cell (iPSC)-Based Neurodegenerative Disease Models for Phenotype Recapitulation and Drug Screening. *Molecules* **25**, (2020).

73. Garcia-Leon JA, Vitorica J, Gutierrez A. Use of human pluripotent stem cell-derived cells for neurodegenerative disease modeling and drug screening platform. *Future Med Chem* **11**, 1305-1322 (2019).

74. Little D, Ketteler R, Gissen P, Devine MJ. Using stem cell-derived neurons in drug screening for neurological diseases. *Neurobiol Aging* **78**, 130-141 (2019).

75. Papandreou A, Luft C, Barral S, Kriston-Vizi J, Kurian MA, Ketteler R. Automated high-content imaging in iPSC-derived neuronal progenitors. *SLAS Discov* **28**, 42-51 (2023).

76. Celsi F, *et al.* Mitochondria, calcium and cell death: a deadly triad in neurodegeneration. *Biochimica et biophysica acta* **1787**, 335-344 (2009).

77. Guo T, Zhang D, Zeng Y, Huang TY, Xu H, Zhao Y. Molecular and cellular mechanisms underlying the pathogenesis of Alzheimer's disease. *Molecular neurodegeneration* **15**, 40 (2020).

78. Moore DJ, West AB, Dawson VL, Dawson TM. Molecular pathophysiology of Parkinson's disease. *Annual review of neuroscience* **28**, 57-87 (2005).

79. Hansen TE, Johansen T. Following autophagy step by step. *BMC Biol* **9**, 39 (2011).

80. Hundeshagen P, Hamacher-Brady A, Eils R, Brady NR. Concurrent detection of autolysosome formation and lysosomal degradation by flow cytometry in a high-content screen for inducers of autophagy. *BMC Biol* **9**, 38 (2011).

81. Liu Y, Levine B. Autosis and autophagic cell death: the dark side of autophagy. *Cell Death Differ* **22**, 367-376 (2015).

82. Wang Y, *et al.* Cardiac glycosides induce autophagy in human non-small cell lung cancer cells through regulation of dual signaling pathways. *Int J Biochem Cell Biol* **44**, 1813-1824 (2012).

83. Dunn DE, He DN, Yang P, Johansen M, Newman RA, Lo DC. In vitro and in vivo neuroprotective activity of the cardiac glycoside oleandrin from Nerium oleander in brain slice-based stroke models. *J Neurochem* **119**, 805-814 (2011).

84. Wang JKT, *et al.* Cardiac glycosides provide neuroprotection against ischemic stroke: discovery by a brain slice-based compound screening platform. *Proceedings of the National Academy of Sciences of the United States of America* **103**, 10461-10466 (2006).

85. Elmaci İ, Alturfan EE, Cengiz S, Ozpinar A, Altinoz MA. Neuroprotective and tumoricidal activities of cardiac glycosides. Could oleandrin be a new weapon against stroke and glioblastoma? *Int J Neurosci* **128**, 865-877 (2018).

86. Rossignoli G, *et al.* Aromatic l-amino acid decarboxylase deficiency: a patient-derived neuronal model for precision therapies. *Brain* **144**, 2443-2456 (2021).

87. Kirkeby A, Nelander J, Parmar M. Generating regionalized neuronal cells from pluripotency, a step-by-step protocol. *Frontiers in cellular neuroscience* **6**, 64 (2012).

88. Huang da W, Sherman BT, Lempicki RA. Systematic and integrative analysis of large gene lists using DAVID bioinformatics resources. *Nature protocols* **4**, 44-57 (2009).

89. Mi H, *et al.* PANTHER version 16: a revised family classification, tree-based classification tool, enhancer regions and extensive API. *Nucleic acids research* **49**, D394-d403 (2021).

90. Bindea G, *et al.* ClueGO: a Cytoscape plug-in to decipher functionally grouped gene ontology and pathway annotation networks. *Bioinformatics* **25**, 1091-1093 (2009).

Hit	Source plate	Well	Z score	Compound
1	14	A10	253.64	Oxyphenbutazone
2	6	D09	152.67	Doxorubicin hydrochloride
3	14	C09	107.82	Thiethylperazine dimalate
4	10	F08	93.28	Alexidine dihydrochloride
5	7	A08	82.75	Daunorubicin hydrochloride
6	9	D07	60.76	Beta-Escin
7	15	F02	57	Topotecan
8	9	B07	53.24	Lanatoside C
9	12	A04	46.93	Digoxigenin
10	12	E06	39.85	Thonzonium bromide
11	11	B02	32.34	Auranofin
12	8	H11	25.03	Sertindole

13	16	G02	24.93	Epirubicin hydrochloride
14	16	B05	24.49	Tegaserod maleate
15	9	G09	24.39	Benzethonium chloride
16	6	D08	21.69	Digoxin
17	5	G06	21.09	Mitoxantrone dihydrochloride
18	9	G06	19.4	Methyl benzethonium chloride
19	7	G11	18.22	Parthenolide
20	6	D07	17.8	Digitoxigenin
21	5	H08	15.89	Clomiphene citrate (Z,E)
22	9	A11	14.96	Pinaverium bromide
23	4	E07	14.67	Perhexiline maleate
24	13	C07	14.2	Proscillaridin A
25	1	H09	13.55	Thioridazine hydrochloride
26	6	A10	13.41	Amiodarone hydrochloride
27	2	F07	12.87	Astemizole
28	7	E03	11.92	Thiostrepton
29	13	H11	11.5	Pyrvinium pamoate
30	4	H09	10.16	Quinacrine dihydrochloride hydrate
31	5	F06	10.13	Methiothepin maleate
32	10	G08	9.97	Merbromin
33	9	A07	9.16	Oxiconazole Nitrate
34	2	E07	9.1	Mefloquine hydrochloride
35	2	G07	8.59	Tamoxifen citrate
36	5	E09	8.14	Bepridil hydrochloride
37	14	A06	7.55	Sertaconazole nitrate
38	7	H11	7.49	Prenylamine lactate
39	13	A11	7.18	Indatraline hydrochloride
40	5	G07	6.77	GBR 12909 dihydrochloride
41	16	E05	6.53	Benzoxiquine
42	2	G04	6.11	Chlorhexidine
43	4	H04	6.06	Trifluoperazine dihydrochloride
44	6	F08	5.67	Meclozine dihydrochloride
45	3	D11	5.59	Camptothecine (S,+)
46	4	C11	5.49	Fendiline hydrochloride
47	11	A11	5.47	Sulconazole nitrate
48	10	C08	5.44	Aprepitant
49	14	C11	5.42	Vorinostat
50	9	B11	5.37	Avermectin B1a
51	5	E05	4.47	Metergoline
52	13	H02	4.27	Halofantrine hydrochloride
53	9	C07	4.17	Nisoldipine
54	4	H11	4.16	Fluphenazine dihydrochloride
55	1	H12	4	Positive Control
56	15	H11	3.94	Hexachlorophene
57	5	C09	3.91	Chlorprothixene hydrochloride
58	10	G12	3.51	Positive Control
59	7	G02	3.43	Ciclopirox ethanolamine
60	4	G05	3.43	Econazole nitrate
61	12	A12	3.27	Positive Control
62	1	H07	3.13	Dibucaine
63	2	H12	3.12	Positive Control
64	4	H03	3.02	Flunarizine dihydrochloride
65	11	G12	2.91	Positive Control
66	1	A12	2.85	Positive Control
67	11	G07	2.84	Azacytidine-5

68	3	A02	2.84	Isoniazid
69	2	E05	2.83	Tioconazole
70	13	F05	2.79	Sertraline
71	2	G12	2.7	Positive Control
72	1	F12	2.69	Positive Control
73	11	F12	2.68	Positive Control
74	1	A02	2.66	Azaguanine-8
75	1	D12	2.6	Positive Control
76	10	F12	2.59	Positive Control
77	10	H12	2.56	Positive Control
78	6	B05	2.56	Amlodipine
79	16	G05	2.55	Lomerizine hydrochloride
80	11	G03	2.55	Raloxifene hydrochloride
81	5	H10	2.52	Prochlorperazine dimaleate
82	5	G04	2.5	Nicardipine hydrochloride
83	5	H07	2.5	Etoposide
84	2	D12	2.49	Positive Control
85	14	H12	2.48	Positive Control
86	13	F12	2.47	Positive Control
87	6	A11	2.46	Amphotericin B
88	1	C12	2.45	Positive Control
89	16	H11	2.44	Cefprozil
90	11	A12	2.43	Positive Control
91	16	H10	2.3	Desonide
92	14	H06	2.29	Ronidazole
93	1	G12	2.27	Positive Control
94	4	H10	2.26	Clofilium tosylate
95	1	F08	2.25	Benoxinate hydrochloride
96	11	G06	2.24	Simvastatin
97	5	F12	2.2	Positive Control
98	10	B11	2.19	Ebselen
99	10	E12	2.16	Positive Control
100	3	B02	2.14	Tranexamic acid
101	12	A03	2.13	Bemegride
102	16	H12	2.13	Positive Control
103	11	H12	2.11	Positive Control
104	16	G12	2.1	Positive Control
105	12	A08	2.09	Oxybenzone
106	7	H05	2.08	Tolazamide
107	1	B12	2.07	Positive Control
108	4	F12	2.06	Positive Control
109	7	D01	2.04	Positive Control
110	10	A10	2.02	Sulfanilamide
111	12	A09	2	Promethazine hydrochloride
112	5	C12	1.99	Positive Control
113	12	B03	1.98	Flubendazol
114	2	C12	1.97	Positive Control
115	10	B12	1.87	Positive Control
116	8	H07	1.86	Penciclovir
117	11	B12	1.86	Positive Control
118	7	H04	1.86	Pentamidine isethionate
119	12	A01	1.83	Positive Control
120	6	B10	1.82	Bisacodyl
121	1	F04	1.8	Triflupromazine hydrochloride
122	5	C08	1.79	Thioguanosine

123	15	H12	1.77	Positive Control
124	9	A03	1.76	Gefitinib
125	16	H08	1.75	Triclabendazole
126	8	H12	1.74	Positive Control
127	7	A05	1.73	Benperidol
128	13	D12	1.71	Positive Control
129	2	E12	1.71	Positive Control
130	4	H12	1.71	Positive Control
131	14	E03	1.69	(-)-Eseroline fumarate salt
132	13	D09	1.69	Zuclopenthixol dihydrochloride
133	12	A07	1.69	Clioquinol
134	16	F11	1.67	Ritonavir
135	16	E01	1.67	Positive Control
136	14	F12	1.66	Positive Control
137	1	H08	1.66	Prednisone
138	15	H09	1.65	Sildenafil
139	16	H04	1.64	Raltitrexed
140	16	H03	1.62	Pemetrexed disodium
141	7	H03	1.6	Selegiline hydrochloride
142	3	B01	1.59	Positive Control
143	12	D12	1.59	Positive Control
144	11	A10	1.59	Dichlorphenamide
145	16	D02	1.58	Aminacrine
146	9	H07	1.57	Pramoxine hydrochloride
147	2	B11	1.57	Nocodazole
148	11	D12	1.57	Positive Control
149	7	C12	1.57	Positive Control
150	4	G12	1.55	Positive Control
151	6	H07	1.54	Primaquine diphosphate
152	12	A10	1.54	Diacerein
153	1	C07	1.53	Cimetidine
154	6	H06	1.53	Brompheniramine maleate
155	10	A09	1.51	Sulfadimethoxine
156	1	G10	1.51	Acebutolol hydrochloride
157	1	F11	1.5	Tolazoline hydrochloride
158	11	H06	1.5	Reserpine
159	10	H09	1.49	Dienestrol
160	13	E12	1.48	Positive Control
161	16	H07	1.48	Milnacipran hydrochloride
162	11	E12	1.47	Positive Control
163	10	H10	1.47	Pridinol methanesulfonate salt
164	16	H05	1.47	Ceftibuten
165	6	H09	1.46	Felodipine
166	10	A04	1.46	Phenethicillin potassium salt
167	10	H11	1.45	Amrinone
168	7	D12	1.45	Positive Control
169	8	H05	1.43	Tomoxetine hydrochloride
170	10	G10	1.43	Drofenine hydrochloride
171	13	H06	1.42	Molindone hydrochloride
172	10	G03	1.42	Podophyllotoxin
173	16	D12	1.42	Positive Control
174	10	D12	1.42	Positive Control
175	2	H11	1.41	Gentamicine sulfate
176	12	C12	1.41	Positive Control
177	15	H08	1.4	Rivastigmine

178	8	H10	1.4	Etoricoxib
179	11	A09	1.39	Furazolidone
180	1	G08	1.39	Miconazole
181	5	D12	1.39	Positive Control
182	15	G12	1.38	Positive Control
183	1	H11	1.37	Trimethobenzamide hydrochloride
184	8	H09	1.37	Dexfenfluramine hydrochloride
185	6	A05	1.36	Idebenone
186	1	H06	1.35	Adiphenine hydrochloride
187	6	B01	1.34	Positive Control
188	16	E12	1.33	Positive Control
189	13	C12	1.33	Positive Control
190	1	E12	1.33	Positive Control
191	5	F07	1.33	Clofazimine
192	10	C09	1.32	Monensin sodium salt
193	13	H07	1.32	Alcuronium chloride
194	13	G04	1.32	Isometheptene mucate
195	8	H04	1.3	Thiorphan
196	13	C10	1.3	Chlormadinone acetate
197	3	A03	1.3	Pentylenetetrazole
198	1	F09	1.28	Oxethazaine
199	14	H09	1.26	Cefepime hydrochloride
200	11	A07	1.25	Trimipramine maleate salt

Supplementary Table 10. ATG differential gene expression in Day 65 mDA Patient 02 cultures after CRISPR correction and compound treatments.

ATG	Patient 02 vs (Controls 01 and 02)		CRISPR 01 vs Patient 02		Digoxin-treated line vs Patient 02		Torin 1-treated vs Patient 02	
	FC	*P*-Value	FC	*P*-Value	FC	*P*-Value	FC	*P*-Value
AMBRA1	0.43706262 (down)	6.14E-04	0.7145338 (down)	0.16574542	1.2240671 (up)	0.487703	0.8595378 (down)	0.7000872
ATG12	1.0688772 (no change)	0.792146	1.1249504 (up)	0.10514027	0.92068404 (down)	0.61909074	1.168334 (up)	0.33339965
ATG13	0.9291793 (down)	0.7693057	0.93510157 (down)	0.5057616	0.4419558 (down)	0.0680989	0.90944344 (down)	0.42617658
ATG14	1.1413882 (up)	0.5587088	Not mapped	Not mapped	0.6088769 (down)	0.17958279	Not mapped	Not mapped
ATG16L1	0.59600216 (down)	0.31001356	1.0367168 (no change)	0.9407053	2.9104712 (up)	0.00144182	1.3612424 (up)	0.54965794
ATG16L2	0.71721536 (down)	0.010059934	Not mapped	Not mapped	Not mapped	Not mapped	1.1957258 (up)	0.6599298
ATG2A	0.9201323 (down)	0.8116482	1.986146 (up)	0.16611445	1.2601732 (up)	0.6257956	1.1654925 (up)	0.7045777
ATG2B	0.81731015 (down)	0.24680214	1.335941 (up)	0.35303855	2.0343752 (up)	0.04702732	1.1501077 (up)	0.5015331
ATG3	0.84620136 (down)	0.44752243	Not mapped	Not mapped	1.0925838 (no change)	0.8455659	0.81203955 (down)	0.6288875
ATG4B	1.6198123 (up)	0.5479161	0.7977216 (down)	0.29556963	0.5249194 (down)	0.4338038	0.3615233 (down)	0.00814244
ATG5	2.085391 (up)	0.01342523	Not mapped	Not mapped	0.5981643 (down)	0.27420387	0.73430216 (down)	0.37415075
BECN1	4.088446 (up)	0.19371912	0.43691146 (down)	0.5124709	0.09202237 (down)	0.21182562	0.15318666 (down)	0.28554642
EPG5	0.891338 (down)	0.8618909	1.0892509 (no change)	0.6674719	2.3882854 (up)	0.17077148	1.0209918 (no change)	0.8568484
GABARAP	1.0952392 (no change)	0.78651476	0.89669627 (down)	0.6855389	0.60620856 (down)	0.08376524	1.1691217 (up)	0.5665487
GABARAPL1	0.8820572 (down)	0.5491498	1.0306478 (no change)	0.85970575	1.750449 (up)	0.12943085	1.3634212 (up)	0.24656725
GABARAPL2	0.9287938 (down)	0.82963806	0.8410031 (down)	0.62539303	0.75546306 (down)	0.20855312	1.3366152 (up)	0.37566233
MAP1LC3A	0.8614579 (down)	0.6068979	1.5705838 (up)	0.20977472	1.4284861 (up)	0.01311642	1.3044173 (up)	0.02771006
MAP1LC3B	0.9986874 (down)	0.99608976	0.7477211 (down)	0.19170646	1.5358086 (up)	0.48995838	0.87073094 (down)	0.72981685
RAB24	1.0563483 (no change)	0.7662744	Not mapped	Not mapped	Not mapped	Not mapped	Not mapped	Not mapped
RAB7A	0.91218925 (down)	0.57352966	0.97811717 (down)	0.91971004	1.3447509 (up)	0.07130751	1.143196 (up)	0.4439764
ULK1	0.6885398 (down)	0.32386762	2.6435022 (up)	0.00500735	0.46201056 (down)	0.03606971	2.4438975 (up)	0.00704683
ULK2	1.6028628 (up)	0.43187773	1.4053199 (up)	0.04052436	0.5006925 (down)	0.01474166	1.067213 (no change)	0.8066371
UVRAG	0.16716082 (down)	1.77E-05	2.3673134 (up)	0.05409699	3.923307 (up)	0.00618942	2.1328526 (up)	0.03366591
WIPI1	1.1785417 (up)	0.62346715	0.43872187 (down)	0.01289181	0.5140383 (down)	0.01987111	1.1200486 (up)	0.5993699
WIPI2	0.71252674 (down)	0.025780724	0.6941722 (down)	0.19979995	Not mapped	Not mapped	1.2907548 (up)	0.11014623
WIPI3	0.8958507 (down)	0.6354098	1.0138819 (no change)	0.96299773	0.80224526 (down)	0.4812425	0.9755141 (down)	0.93992513
WDR45	2.1794524 (up)	0.051202912	Not mapped	Not mapped	Not mapped	Not mapped	Not mapped	Not mapped

Genes marked in blue show consistent under- or over-expression when comparing the Patient 02 untreated mDA line profiles with the corresponding CRISPR-corrected and compound-treated ones. Many known ATGs were interrogated. *P*-value and fold change cut-offs were not applied for this analysis; however, some genes have significant *p*- and fold change values in different conditions. ATG= autophagy-related gene, FC= fold change.

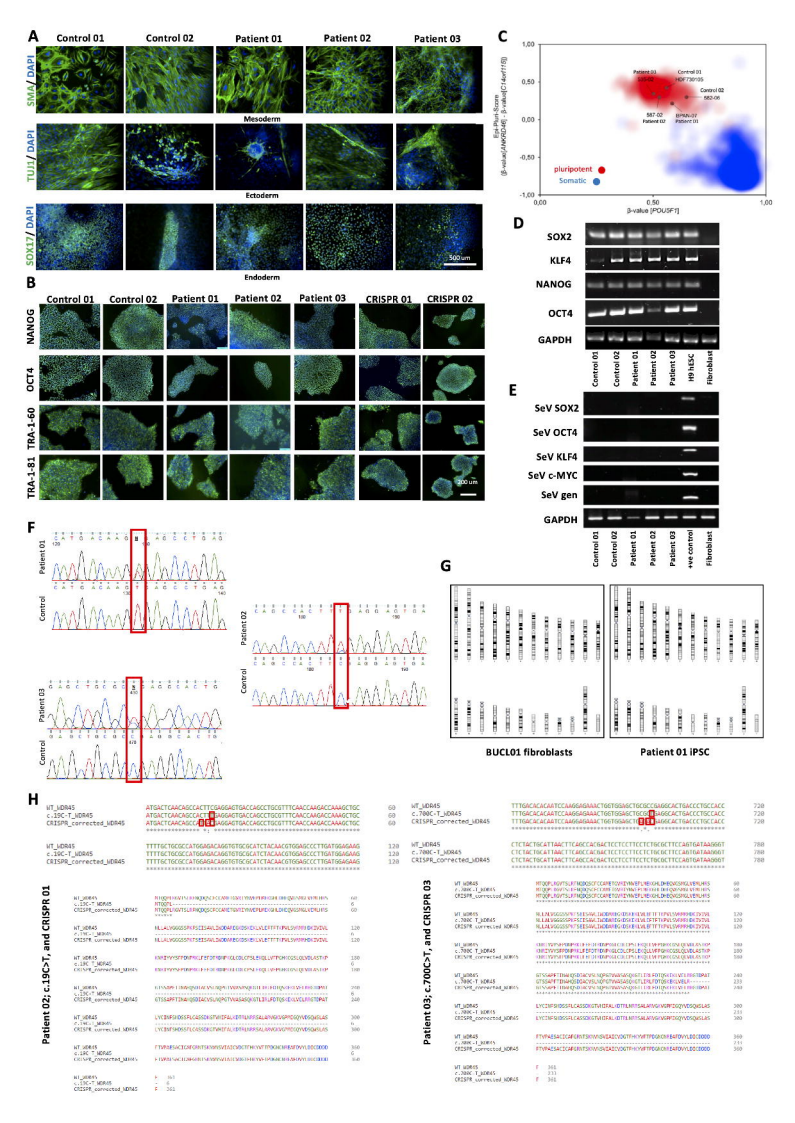
A
Control 01
Control 02
Patient 01
Patient 02
Patient 03
SMA / DAPI
TUJ1 / DAPI
SOX17 / DAPI
Mesoderm
Ectoderm
Endoderm
500 um
B
Control 01
Control 02
Patient 01
Patient 02
Patient 03
CRISPR 01
CRISPR 02
NANOG
OCT4
TRA-1-60
TRA-1-81
200 um
C
Epi-Pluri-Score
[β-value(ANKRD46)] - [β-value(C14orf119)]
β-value [POU5F1]
pluripotent
Somatic
D
SOX2
KLF4
NANOG
OCT4
GAPDH
Control 01
Control 02
Patient 01
Patient 02
Patient 03
H9 hESC
Fibroblast
E
SeV SOX2
SeV OCT4
SeV KLF4
SeV c-MYC
SeV gen
GAPDH
Control 01
Control 02
Patient 01
Patient 02
Patient 03
+ve control
Fibroblast
F
Patient 01
Control
Patient 02
Control
Patient 03
Control
G
BUCL01 fibroblasts
Patient 01 iPSC
H
Patient 02; c.19C>T, and CRISPR 01
Patient 03; c.700C>T, and CRISPR 03

Term	Pathways	Count	PValue	Genes
GO:0030574	collagen catabolic process	8	4.13E-11	COL1A1, COL18A1, COL3A1, COL1A2, COL5A1, COL4A1, MMP2, COL5A2
GO:0030198	extracellular matrix organization	8	1.09E-07	COL1A1, COL18A1, COL3A1, COL1A2, COL5A1, COL4A1, COL5A2, ICAM5
GO:0071230	cellular response to amino acid stimulus	6	3.61E-08	COL1A1, COL3A1, COL1A2, COL4A1, MMP2, COL5A2
GO:0030199	collagen fibril organization	5	1.10E-06	COL1A1, COL3A1, COL1A2, COL5A1, COL5A2
GO:0007155	cell adhesion	5	0.013360993	PTPRT, COL1A1, COL18A1, COL5A1, ICAM5
GO:0050776	regulation of immune response	4	0.005505298	COL1A1, COL3A1, COL1A2, ICAM5
GO:0001525	angiogenesis	4	0.010211886	COL18A1, EPAS1, MMP2, EIF2AK3
GO:0030168	platelet activation	3	0.022615229	COL1A1, COL3A1, COL1A2
GO:0007156	homophilic cell adhesion	3	0.040550022	PTPRT, PCDHGA10, CDHR2
GO:1903225	endodermal cell differentiation	2	0.004045568	COL5A1, COL5A2
GO:0001957	ossification	2	0.012089103	COL1A1, MMP2
GO:0032964	collagen biosynthetic process	2	0.012089103	COL1A1, COL5A1
GO:0060346	bone trabecula formation	2	0.016087191	COL1A1, MMP2
GO:0043589	skin morphogenesis	2	0.018080341	COL1A1, COL1A2
GO:0043206	extracellular fibril organization	2	0.024036308	COL3A1, COL5A1
GO:0070208	protein heterotrimerization	2	0.027987456	COL1A1, COL1A2
KEGG:hsa04974	Protein digestion and absorption	7	4.08E-08	COL1A1, COL18A1, COL3A1, COL1A2, COL5A1, COL4A1, COL5A2
KEGG:hsa04512	ECM-receptor interaction	6	1.58E-06	COL1A1, COL3A1, COL1A2, COL5A1, COL4A1, COL5A2
KEGG:hsa04510	Focal adhesion	6	1.06E-04	COL1A1, COL3A1, COL1A2, COL5A1, COL4A1, COL5A2
KEGG:hsa04151	PI3K-Akt signaling pathway	6	0.001156253	COL1A1, COL3A1, COL1A2, COL5A1, COL4A1, COL5A2
KEGG:hsa04611	Platelet activation	5	2.39E-04	COL1A1, COL3A1, COL1A2, COL5A1, COL5A2
KEGG:hsa04216	Ferroptosis	2	0.023182938	ACSL6, SLC40A1
KEGG:hsa04722	Neurotrophin signaling pathway	2	0.02438856	ARHGDIG, MAPK7
KEGG:hsa05418	Fluid shear stress and atherosclerosis	2	0.038744049	MAPK7, MMP2

A

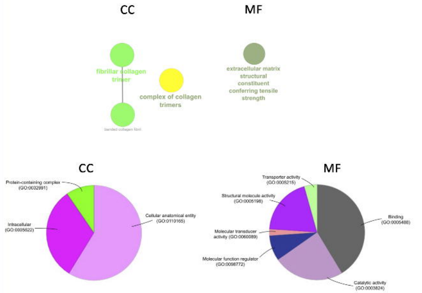

B GO enriched terms in Patients vs (Controls & CRISPR)

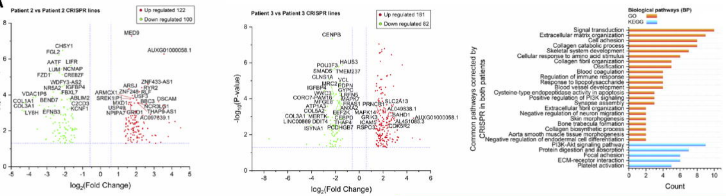

C

Term	Pathways	Count	PValue	Genes
GO				
GO:0007165	Signal transduction	10	0.047346097	PTPRT, EXT1, THBD, MAPK7, CRABP2, IGFBP4, ARAP2, PDE7B, JAK2, TEX2
GO:0030198	Extracellular matrix organization	9	1.36E-06	COL1A1, COL18A1, COL3A1, COL1A2, COL5A1, COL4A1, COL5A2, ICAM5, DCN
GO:0030574	Collagen catabolic process	8	7.47E-09	COL1A1, COL18A1, COL3A1, COL1A2, COL5A1, COL4A1, MMP2, COL5A2
GO:0007155	Cell adhesion	8	0.002727335	PTPRT, COL1A1, COL18A1, DSCAM, COL5A1, CDH11, ICAM5, AATF
GO:0001501	Skeletal system development	7	2.08E-05	EXT1, COL1A1, COL3A1, COL1A2, IGFBP4, CDH11, COL5A2
GO:0071230	Cellular response to amino acid stimulus	6	1.36E-06	COL1A1, COL3A1, COL1A2, COL4A1, MMP2, COL5A2
GO:0001957	Ossification	5	0.024406307	COL1A1, MMP2, EXT1, CDH11, COL5A2
GO:0030199	Collagen fibril organization	5	1.93E-05	COL1A1, COL3A1, COL1A2, COL5A1, COL5A2
GO:0001568	Blood vessel development	4	5.05E-04	COL1A1, COL1A2, COL5A1, AHR
GO:0032496	Response to lipopolysaccharide	4	0.029975494	THBD, NGFR, JAK2, DCN
GO:0050776	Regulation of immune response	4	0.03686949	COL1A1, COL3A1, COL1A2, ICAM5
GO:0007596	Blood coagulation	4	0.040052815	COL1A1, THBD, COL1A2, JAK2
GO:0007416	Synapse assembly	3	0.026058814	KIRREL3, DSCAM, NRG1
GO:0014068	Positive regulation of PI3K signaling	3	0.029310436	NRG1, JAK2, DCN
GO:0006919	Cysteine-type endopeptidase activity in apoptosis	3	0.045755158	NGFR, JAK2, BBC3
GO:1903225	Negative regulation of endodermal cell differentiation	2	0.008201558	COL5A1, COL5A2
GO:0060414	Aorta smooth muscle tissue morphogenesis	2	0.012277442	COL3A1, PROX1
GO:0032964	Collagen biosynthetic process	2	0.024406307	COL1A1, COL5A1
GO:0060346	Bone trabecula formation	2	0.032410549	COL1A1, MMP2
GO:0043589	Skin morphogenesis	2	0.036388366	COL1A1, COL1A2
GO:2001223	Negative regulation of neuron migration	2	0.036388366	COL3A1, NRG1
GO:0043206	Extracellular fibril organization	2	0.048225371	COL3A1, COL5A1
KEGG				
KEGG:hsa04151	PI3K-Akt signaling pathway	9	6.26E-05	COL1A1, NGFR, COL3A1, COL1A2, COL5A1, COL4A1, COL5A2, DDIT4, JAK2
KEGG:hsa04974	Protein digestion and absorption	7	1.38E-06	COL1A1, COL18A1, COL3A1, COL1A2, COL5A1, COL4A1, COL5A2
KEGG:hsa04512	ECM-receptor interaction	6	2.69E-05	COL1A1, COL3A1, COL1A2, COL5A1, COL4A1, COL5A2
KEGG:hsa04510	Focal adhesion	6	0.001515246	COL1A1, COL3A1, COL1A2, COL5A1, COL4A1, COL5A2
KEGG:hsa04611	Platelet activation	5	0.002005127	COL1A1, COL3A1, COL1A2, COL5A1, COL5A2

D

Term	Pathways	Count	PValue	Genes
GO				
GO:0030198	extracellular matrix organization	21	1.85E-14	COL14A1, LUM, FN1, HSD17B12, LAMC1, THBS1, FBLN5, COL1A1, COL3A1, VCAN, COL1A2, COL5A1, LOX, COL4A1, COL5A2, ITGAV, TGFBI, COL9A2, CD44, JAM3, FBN1
GO:0043066	negative regulation of apoptotic process	11	0.021860737	PDGFRB, ANXA1, PLK2, PDE3A, TAX1BP1, VEGFB, SPRY2, RPS27A, THBS1, CD44, MCL1
GO:0030199	collagen fibril organization	9	5.79E-09	COL1A1, COL3A1, TGFB2, COL1A2, COL5A1, LOX, LUM, COL14A1, COL5A2
GO:0001525	angiogenesis	9	0.002464836	TGFB2, MCAM, MMP2, VEGFB, FN1, ACKR3, ITGAV, TGFBI, JAM3
GO:0001649	osteoblast differentiation	8	1.11E-04	COL1A1, WWTR1, VCAN, GJA1, DHX9, CCDC47, PENK, RBMX
GO:0030574	collagen catabolic process	7	5.52E-05	COL1A1, COL3A1, COL1A2, COL5A1, COL4A1, MMP2, COL5A2
GO:0071230	cellular response to amino acid stimulus	6	1.28E-04	COL1A1, COL3A1, COL1A2, COL4A1, MMP2, COL5A2
GO:0007179	TGFβ receptor signaling pathway	6	0.002818184	KLF10, COL3A1, TGFB2, COL1A2, ADAM9, RPS27A
GO:0006457	protein folding	6	0.041207939	CCT2, PPIL1, VBP1, DNAJA2, FKBP1B, CCT4
GO:0006120	mitochondrial electron transport	4	0.014654336	NDUFB9, NDUFA4, NDUFA3, NDUFC2
GO:0051592	response to calcium ion	4	0.022927328	PENK, ADAM9, ANXA7, THBS1
KEGG				
KEGG:hsa04151	PI3K-Akt signaling pathway	16	3.02E-05	PDGFRB, VEGFB, FN1, LAMC1, GNG12, GNG11, THBS1, COL1A1, COL3A1, COL1A2, COL5A1, COL4A1, COL5A2, DDIT4, ITGAV, MCL1
KEGG:hsa04510	Focal adhesion	13	1.18E-05	PDGFRB, VEGFB, FN1, LAMC1, THBS1, COL1A1, PPP1CC, COL3A1, COL1A2, COL5A1, COL4A1, COL5A2, ITGAV
KEGG:hsa04512	ECM-receptor interaction	11	1.39E-07	COL1A1, COL3A1, COL1A2, COL5A1, COL4A1, COL5A2, FN1, ITGAV, LAMC1, THBS1, CD44
KEGG:hsa05016	Huntington's disease	8	0.011850365	NDUFB9, NDUFA4, NDUFA3, NDUFC2, UQCRC2, COX5B, SLC25A5, BBC3
KEGG:hsa05012	Parkinson's disease	7	0.009945243	NDUFB9, NDUFA4, NDUFA3, NDUFC2, UQCRC2, COX5B, SLC25A5
KEGG:hsa04514	Cell adhesion molecules	6	0.036414167	VCAN, HLA-B, HLA-C, ITGAV, CLDN1, JAM3
KEGG:hsa04932	Non-alcoholic fatty liver disease	6	0.045484783	NDUFB9, NDUFA4, NDUFA3, NDUFC2, UQCRC2, COX5B

E

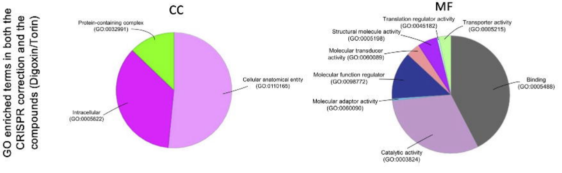

F

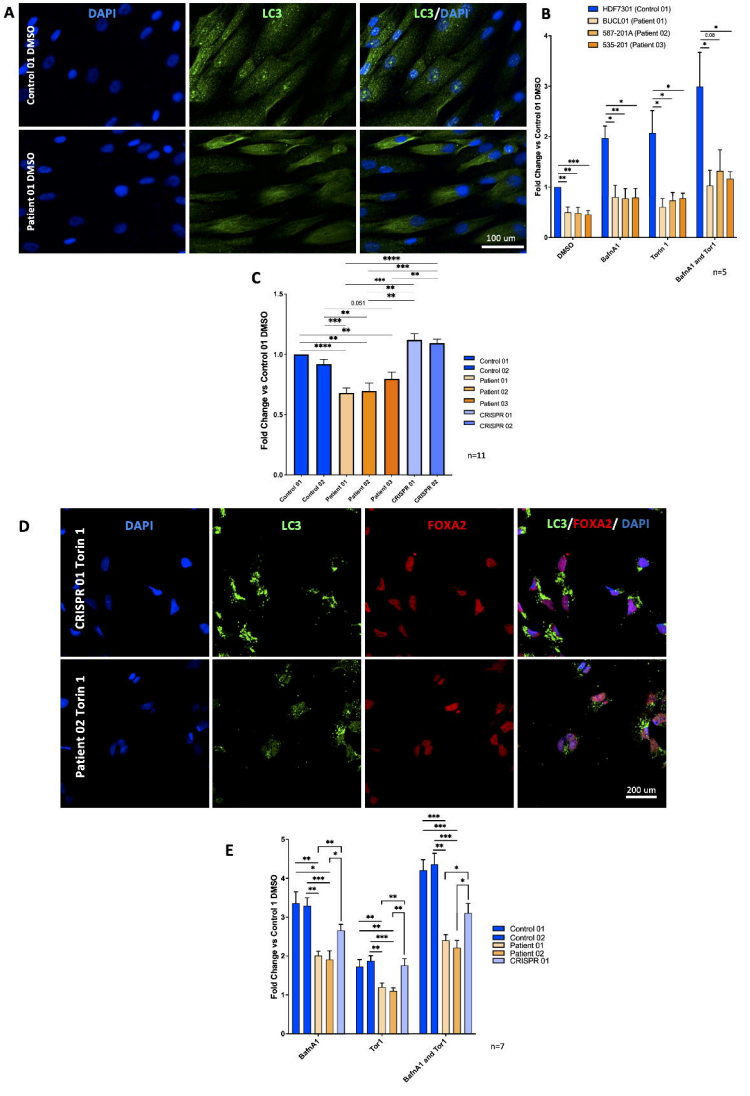
A
DAPI
LC3
LC3/DAPI
Control 01 DMSO
Patient 01 DMSO
100 um
B
HDF7301 (Control 01)
BUCL01 (Patient 01)
587-201A (Patient 02)
535-201 (Patient 03)
Fold Change vs Control 01 DMSO
DMSO
BafnA1
Torin 1
BafnA1 and Tor1
n=5
C
Fold Change vs Control 01 DMSO
Control 01
Control 02
Patient 01
Patient 02
Patient 03
CRISPR 01
CRISPR 02
n=11
D
DAPI
LC3
FOXA2
LC3/FOXA2/ DAPI
CRISPR 01 Torin 1
Patient 02 Torin 1
200 um
E
Fold Change vs Control 1 DMSO
Control 01
Control 02
Patient 01
Patient 02
CRISPR 01
BafnA1
Tor1
BafnA1 and Tor1
n=7

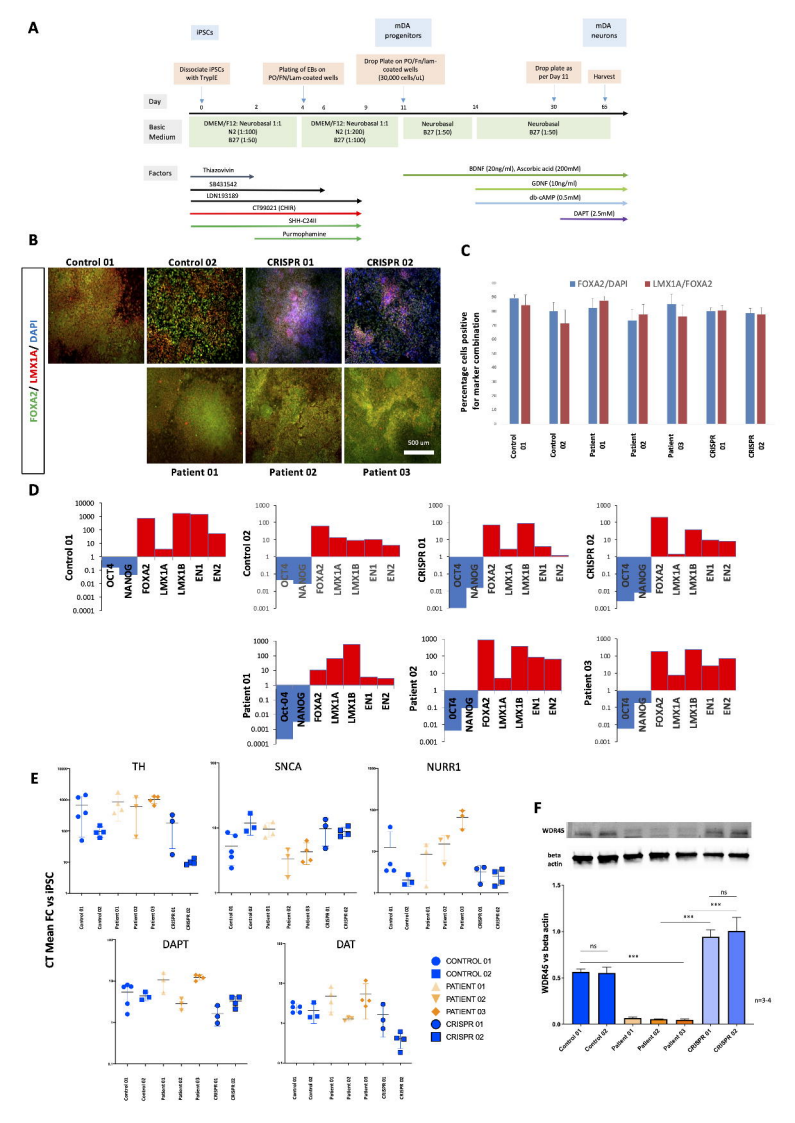
A
iPSCs
mDA progenitors
mDA neurons
Dissociate iPSCs with TrypLE
Plating of EBs on PO/FN/Lam-coated wells
Drop Plate on PO/Fn/lam-coated wells (30,000 cells/uL)
Drop plate as per Day 11
Harvest
Day
0
2
4
6
9
11
14
30
65
Basic Medium
DMEM/F12: Neurobasal 1:1 N2 (1:100) B27 (1:50)
DMEM/F12: Neurobasal 1:1 N2 (1:200) B27 (1:100)
Neurobasal B27 (1:50)
Neurobasal B27 (1:50)
Factors
Thiazovivin
SB431542
LDN193189
CT99021 (CHIR)
SHH-C24II
Purmophamine
BDNF (20ng/ml), Ascorbic acid (200mM)
GDNF (10ng/ml)
db-cAMP (0.5mM)
DAPT (2.5mM)
B
Control 01
Control 02
CRISPR 01
CRISPR 02
FOXA2/ LMX1A/ DAPI
500 um
Patient 01
Patient 02
Patient 03
C
FOXA2/DAPI
LMX1A/FOXA2
Percentage cells positive for marker combination
Control 01
Control 02
Patient 01
Patient 02
Patient 03
CRISPR 01
CRISPR 02
D
Control 01
Control 02
CRISPR 01
CRISPR 02
Patient 01
Patient 02
Patient 03
OCT4
NANOG
FOXA2
LMX1A
LMX1B
EN1
EN2
E
TH
SNCA
NURR1
DAPT
DAT
CT Mean FC vs iPSC
CONTROL 01
CONTROL 02
PATIENT 01
PATIENT 02
PATIENT 03
CRISPR 01
CRISPR 02
F
WDR45
beta actin
WDR45 vs beta actin
ns
***
n=3-4
Control 01
Control 02
Patient 01
Patient 02
Patient 03
CRISPR 01
CRISPR 02